

# TITANIUM(IV)–EDTA COMPLEX

## Kinetics of thermal decomposition by non-isothermal procedures

Luciana S. Guinesi, C. A. Ribeiro\*, Marisa S. Crespi, A. F. Santos and Marisa V. Capela

Universidade Estadual Paulista/UNESP, Instituto de Química, Departamento de Química Analítica, P.O. Box 355, 14801-970 Araraquara, SP, Brazil

This work aims the evaluation of the kinetic triplets corresponding to the two successive steps of thermal decomposition of Ti(IV)–ethylenediaminetetraacetate complex. Applying the isoconversional Wall–Flynn–Ozawa method on the DSC curves, average activation energy:  $E=172.4\pm 9.7$  and  $205.3\pm 12.8$  kJ mol<sup>-1</sup>, and pre-exponential factor:  $\log A=16.38\pm 0.84$  and  $18.96\pm 1.21$  min<sup>-1</sup> at 95% confidence interval could be obtained, regarding the partial formation of anhydride and subsequent thermal decomposition of uncoordinated carboxylate groups, respectively.

From  $E$  and  $\log A$  values, Dollimore and Málek methods could be applied suggesting PT (Prout–Tompkins) and R3 (contracting volume) as the kinetic model to the partial formation of anhydride and thermal decomposition of the carboxylate groups, respectively.

**Keywords:** activation energy, kinetic model, non-isothermal kinetics, Ti(IV)–EDTA, TiO<sub>2</sub>

### Introduction

#### Solid Ti(IV)–EDTA complex

Despite the fact the great number of complexes between ethylenediaminetetraacetic acid (EDTA) and metals ions described in literature, there are few studies regarding to the complexes of Ti(IV)–EDTA in the solid-state. Sawyer and McKinnie [1] suggested the formation of the solid TiOH<sub>2</sub>EDTA·H<sub>2</sub>O and they observed, through infrared spectra, that the TiO<sup>2+</sup> ion was covalently bonded to only two carboxylate groups of the ligand.

The TiO(EDTAH<sub>2</sub>)·H<sub>2</sub>O compound was obtained by Kristine *et al.* [2] by mixing the stoichiometric amounts of disodium EDTA salt and TiO<sup>2+</sup> ion in solution after adjustment the pH to 1.5. The structural nature of TiO(EDTA)<sup>2-</sup> in solution and its reaction with H<sub>2</sub>O<sub>2</sub> forming TiO<sub>2</sub>(EDTA)<sup>2-</sup> was studied at pH 2.0–5.2.

Fackler *et al.* [3] suggested, through X-ray diffraction, the formation of the pentacoordinated compound [Ti(EDTA)(H<sub>2</sub>O)] with a geometric structure of a pentagonal-bipyramid.

Studies concerning the thermal behavior and mainly the obtainment of the kinetic triplet to thermal decomposition reaction had not been reported.

#### Kinetics aspects

The rate law for a solid-state process can be expressed by a simple differential kinetic equation [4]:

$$\frac{d\alpha}{dt} = A \exp\left(-\frac{E}{RT}\right) f(\alpha) \quad (1)$$

where  $A$  is the preexponential factor,  $E$  is the activation energy,  $R$  is the gas constant and  $f(\alpha)$  is an algebraic expression of kinetic model as a function of fractional conversion  $\alpha$  ( $0\leq\alpha\leq 1$ ). The Arrhenius parameters should not depend on the temperature  $T$  and the fractional conversion  $\alpha$  [4]. For dynamic data obtained at a constant heating rate,  $\beta=dT/dt$ , this new term is inserted in the Eq. (1) to obtain the transformation [5]:

$$\frac{d\alpha}{dt} = \frac{A}{\beta} \exp\left(\frac{-E}{RT}\right) f(\alpha) \quad (2)$$

This rather trivial transformation presents a great physical meaning. It implicitly assumes that the change in experimental conditions from isothermal to non-isothermal does not affect the reaction kinetics. Intuitively, this assumption feels quite reasonable, at least as long as we are dealing with a single-step process. Non-isothermal heating resolved a major problem of the isothermal experiment, which is that a sample requires some time to reach the experimental temperature undergoing some transformations that are likely to affect the results of the following kinetic analysis. This problem especially restricts the use of high temperatures in isothermal experiments [6]. The kinetic analysis through isoconversional methods support the principle that reaction rate at a constant extent of conversion  $\alpha$  is only function of temperature [6]. The isoconversional method of Flynn, Wall and Ozawa for evaluating the activation energy uses the integral form of Eq. (2) to obtain the transformation [5–7]:

$$g(\alpha) = \frac{A}{\beta} \int_0^T \exp\left(-\frac{E}{RT}\right) dT = \frac{AE}{\beta R} p(x) \quad (3)$$

\* Author for correspondence: ribeiroc@iq.unesp.br

where  $x=(E/RT)$ . For  $p(x)$ , where  $20 \leq x \leq 60$ , we can use the Doyle's approximation of the integral temperature [5, 7, 8]:

$$\log p(x) \cong -2.315 - 0.4567x \quad (4)$$

However, a simpler expression has been developed by the substitution of Eq. (4) into Eq. (3) to obtain [5, 7]:

$$\log g(\alpha) \cong \log \frac{AE}{R} - \log \beta - 2.315 - 0.457 \frac{E}{RT} \quad (5)$$

Then, from the slope of a plot of  $\log \beta$  vs.  $1/T$  the activation energy can be calculated to fixed values of  $\alpha$  from experiments at different heating rates testing the constancy of  $E$  with respect to  $\alpha$  and  $T$  [5–7]. The pre-exponential factor is evaluated taking into account that the reaction is a first-order one and can be defined as [5]:

$$A = \frac{\beta E}{RT_m^2} \exp\left(\frac{E}{RT_m}\right) \quad (6)$$

#### Kinetic model determination

The rate of the kinetic process  $d\alpha/dt$  through DSC curves is based on the relation:

$$\frac{d\alpha}{dt} = \frac{\phi}{\Delta H_c} \quad (7)$$

where  $\phi$  is the heat flow normalized per sample mass and  $\Delta H_c$  corresponds to the enthalpy change associated with this process [4, 9, 10].

The shape of a dynamic DSC curve at a specific heating rate considering any kind of model can be written as [9, 10]:

$$\phi = \Delta H_c A \exp\left(-\frac{E_a}{RT}\right) f(\alpha) \quad (8)$$

The test to find the kinetic model proposed by Málek is based on this equation and on the normalized  $y(\alpha)$  and  $z(\alpha)$  functions, that, under non-isothermal conditions, they are given by:

$$y(\alpha) = \phi \exp\left(\frac{E_a}{RT}\right) = B_n f(\alpha) \quad (9)$$

where  $B_n = \Delta H_c A$  is constant and the shape of the  $y(\alpha)$  function is formally identical to the kinetic model  $f(\alpha)$  in which the maximum value is  $\alpha_y^*$ .

$$z(\alpha) = \phi T \pi \left(\frac{E_a}{RT}\right) = \Delta H_c \beta f(\alpha) g(\alpha) \quad (10)$$

where  $\pi(E_a/RT)$  is an approximation of the integral temperature that, in case of the  $z(\alpha)$  function, can be obtained accurately considering the approximation  $\pi \approx RT/E_a$ , then:

$$z(\alpha) = \phi T^2 = C_n f(\alpha) g(\alpha) \quad (11)$$

where  $C_n = \Delta H_c \beta E_a / R$  is constant and the  $\alpha$  at the maximum of the  $z(\alpha)$ ,  $\alpha_z^*$ , is characteristic for any kinetic model [4, 9, 10]. The fractional conversion  $\alpha$  can be easily obtained by partial integration of isothermal or non-isothermal TA curve [10].

The kinetic models to some thermal decomposition reactions can also be obtained through Dollimore's method, which is based on the 'sharpness' of the onset ( $T_i$ ) and final ( $T_f$ ) temperatures of the TG/DTG and its asymmetry. The investigation of some parameters that describe this asymmetry can thereby indicate the probable kinetic mechanism expressed as  $f(\alpha)$ . When the thermal decomposition reaction is not complex, the quantitative approach may be obtained using parameters such as  $\alpha_{\max}$  or  $(d\alpha/dT)_{\max}$ , peak temperature ( $T_p$ ) and half width from DTG curves [11, 12].

This work aims the kinetic evaluation of  $E$ ,  $A$  and  $f(\alpha)$  to the partial formation of anhydride and thermal decomposition of the carboxylate groups of Ti(IV)–EDTA complex through the non isothermal methods described, based on the TG, DTG and DSC curves. The kinetic model exercises great influence on the morphological properties to  $\text{TiO}_2$  obtained at  $1200^\circ\text{C}$  like as homogeneity, porosity and surface-to-volume ratio which are fundamental in the gas sensor performance device [13, 14].

## Experimental

### Chemicals

The metal, inorganic salts and acids used to prepare the complex were reagent grade. EDTA in acid form and metallic titanium were purchased from Analyticals-Carlo Erba Co. Ammonium carbonate, chlorid, nitrate and sulphuric acids were purchased from Merck. Anhydrous ethanol was previously purified in our labor.

### Preparation of the solid titanium(IV)–EDTA complex

2.729 mmol of metallic titanium was dissolved in a minimum quantity of hot concentrated chloric acid to obtain  $\text{TiCl}_3$  in the medium HCl which was oxidized to  $\text{TiOCl}_2$  by further addition of drops of sulphonic solution. It was added, at room temperature and under constant stirring, to an equimolar aqueous solution of ammonium salt from EDTA maintained at pH 1.5. The system was left still for 1 h at room temperature and the precipitate was filtered, washed in hot distilled water so that anions and ligand excess could be eliminated, dried in an oven at  $60^\circ\text{C}$  and stored in a desiccator which contained anhydrous calcium chloride. The obtained

compound was the  $\text{TiO}(\text{NCH}_2(\text{CH}_2\text{COO})_2\text{H})_2$  (Mchelate)=354.13 g mol<sup>-1</sup>, yields =80%. Calculated: C, 33.92%; N, 7.91%; H, 3.98%. Found: C, 33.75%; N, 7.82%; H, 4.08%.

### Characterization

The complex was characterized through infrared absorption spectra (IR) in the 4000–200 cm<sup>-1</sup> region by using a Spectrum 2000 spectrophotometer as CsI pellet and through elemental analysis (N, H, C) by using CE Instruments equipment, model EA 1110-CHNS-O. The residue oxide was characterized through DRX using a Siemens D 5000 diffractometer with CuK<sub>α</sub> radiation, submitted to 40 kV, 30 mA, 0.05° s<sup>-1</sup> step and exposed to radiation from 4 up to 70° (2θ). The TG/DTG-DTA experiments were performed using a simultaneous module of thermal analysis, SDT 2960 from TA Instruments, under dynamic atmosphere of nitrogen and synthetic air (100 mL min<sup>-1</sup>), alumina crucible of 40 μL, α-Al<sub>2</sub>O<sub>3</sub> as reference material, sample mass around 6 mg and heating rates of 5, 10 and 20°C min<sup>-1</sup> from 40 up to 1200°C. DSC recording was obtained by using a DSC 2910 module from TA Instruments under dynamic atmosphere of nitrogen (100 mL min<sup>-1</sup>), covered aluminum crucible of 10 μL with sample mass around 2 mg, aluminum crucible as reference material and heating rates of 5, 10 and 20°C min<sup>-1</sup> from 40 up to 600°C. The *E* and log*A* kinetic parameters were calculated through the software's TGAKin V4.04 and DSCASTMKin V4.08 from TA Instruments.

## Results and discussion

The synthesis of the compound was performed at pH 1 in order to avoid the hydrolysis of the titanium ion and the formation of the stable precipitate complex  $\text{TiO}(\text{NCH}_2(\text{CH}_2\text{COO})_2\text{H})_2$ . The  $\text{TiO}^{2+}$  ion form, either in aqueous or alcoholic solutions, decrease the complex solubility with EDTA even at pH 1.5, due to its high stability (p*K* is 12.08±0.02 at ionic strength μ=1.0) [15].

Data from IR spectra to the compound showed three broadening bands with medium intensity at 3330, 3238 and 2941 cm<sup>-1</sup> due to the C–H and O–H stretching in the CH<sub>2</sub> and protonated carboxylate groups from EDTA [1, 16]. Appearance of this peak at 2800–3000 cm<sup>-1</sup> indicates the ligand is N-deprotonated taken as strong evidence for the formation of a chelate [1, 17]. A very strong broadening band which splits in two peaks at 1697 and 1618 cm<sup>-1</sup> are attributed to the anti-symmetrical vibration of C=O, originated from the unbounded protonated carboxylates and carboxylate groups coordinated to  $\text{TiO}^{2+}$  ion, respectively [1, 16, 17]. Medium and weak bands at 1462 and 1082 cm<sup>-1</sup>

have been assigned to C=O symmetric and C–N stretching, respectively [16, 17]. The difference in frequency between the peaks for antisymmetrical and symmetrical vibrations for C=O is less than 225 cm<sup>-1</sup> indicating the bonding TiO-carboxylate is primarily ionic [1]. A strong and sharp band at 934 cm<sup>-1</sup> has been established to be due to Ti=O stretching mode [2]. A medium band at 476 and 438 cm<sup>-1</sup> are associated with ν<sub>Ti–N</sub> and the weaker ones at 394 and 371 cm<sup>-1</sup> with ν<sub>Ti–O</sub> vibrations [18]. From IR spectrum data, TG curves and elemental analysis it could be suggested that the  $\text{TiO}(\text{NCH}_2(\text{CH}_2\text{COO})_2\text{H})_2$  compound as being a penta-coordinated chelate having two uncoordinated carboxylate groups.

The TG and DTA curves of the complex obtained under synthetic air, Fig. 1a, and nitrogen, Fig. 1b, atmospheres at 5°C min<sup>-1</sup> show initial mass loss between 215 and 243°C (1.44%) with an endothermic peak at 234°C under N<sub>2</sub> ascribed to the loss of 0.25H<sub>2</sub>O by rearrangement of protonated carboxylate groups resulting a partial formation of anhydride chelate. The subsequent thermal decomposition is due to the loss of anhydride and carboxylate with evaluation of CO/CO<sub>2</sub> which are thermally less stable compared to the ethylenediamine fraction [19]. These weakest groups are decomposing with two steps of mass loss for each atmosphere: under synthetic air, between 248 and 432°C (56.5%) corresponding to the exothermic peak at 319°C; under nitrogen, between 251 and 400°C (52.8%) with endothermic peaks at 286 and 356°C probably with the evaluation of H<sub>2</sub>O, CO<sub>2</sub> and CO. The remaining compound with the ethylenediamine fraction decomposes into TiO<sub>2</sub> whose formation is verified over 551 and 910°C under synthetic air (22.0%) and nitrogen (22.5%), respectively showing a broad endothermic peak around 800°C. Under inert atmosphere, the partial decomposition of carboxylates allows the

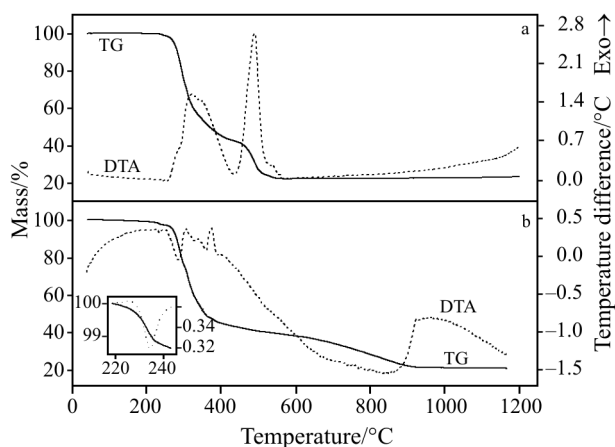


**Fig. 1** TG-DTA curves to the  $\text{TiO}(\text{CH}_2\text{N}(\text{CH}_2\text{COO})_2\text{H})_2$  compound at 5°C min<sup>-1</sup> under the atmospheres: a – synthetic air and b – nitrogen

obtainment of residue oxide which was characterized as tetragonal rutile phase by X-ray diffraction patterns data likewise that from air. Although the identical residue, the thermal decomposition in both atmospheres occurs with a likely dissimilar mechanism, as indicated by the feature of the TG and DTA curves.

#### Calculation of the activation energy and pre-exponential factor

In the TG-DTG curves under nitrogen atmosphere, Fig. 2, it can be seen the mass loss associated to the anhydride (215–253°C) formation and the first step of carboxyl decomposition (251–317°C) at distinct heating rates. The DSC curves, Fig. 3, show the endothermic peaks with similarities to the TG-DTG curves.

The kinetic parameters  $E$  and  $\log A$  for these thermal events were obtained applying the Flynn–Wall–Ozawa method [5–8] on the reaction limits defined by TG-DTG and DSC curves described in Table 1. To each fixed fractional conversion  $\alpha$  and

its correspondent temperatures, the  $E$  parameter results from the slope of the plot of  $\log \beta$  vs.  $1000/T$ , Eq. (5), and then the corresponding  $\log A$  through Eq. (6). Although the consecutive reactions, we are dealing with a single-step process, what allows to select suitable  $\alpha$  range in which an eventual subsequent reaction interferences are not occurring. This criterious  $\alpha$  selection leads to obtained results within the limit to be used the Doyle's approximation to  $p(x)$ , Eq. (4), in which the  $20 \leq E/RT \leq 60$  [8]. Thus, at 95% confidence interval, the average values found to  $E$  and  $\log A$  regarding the partial formation of anhydride are:  $163.0 \pm 4.5$  and  $172.4 \pm 9.7$  kJ mol<sup>-1</sup>,  $16.13 \pm 0.41$  and  $16.38 \pm 0.84$  min<sup>-1</sup>, from TG ( $10.0 \leq \alpha \leq 50.0\%$ ) and DSC ( $5.0 \leq \alpha \leq 50.0\%$ ) curves, respectively. Regarding the thermal decomposition of the uncoordinated carboxylate groups of the complex, the average values obtained to  $E$  and  $\log A$ , through TG ( $25.0 \leq \alpha \leq 70.0\%$ ) and DSC ( $10.0 \leq \alpha \leq 45.0\%$ ) curves are:  $211.2 \pm 1.7$  and  $205.3 \pm 12.8$  kJ mol<sup>-1</sup>,  $19.21 \pm 0.17$  and  $18.96 \pm 1.21$  min<sup>-1</sup>, respectively.

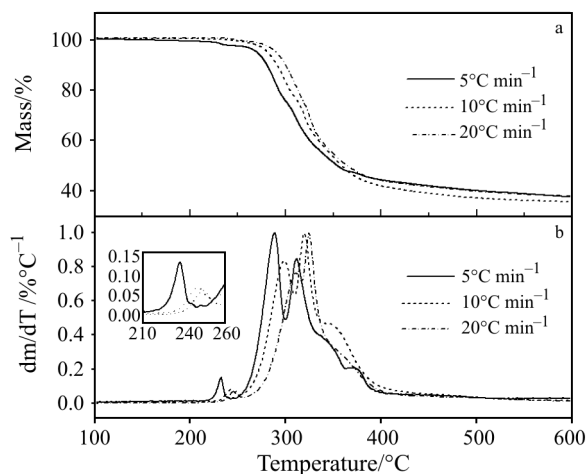


**Fig. 2** a – TG and b – DTG curves to the  $\text{TiO}(\text{CH}_2\text{N}(\text{CH}_2\text{COO})_2\text{H})_2$  compound at several heating rates under nitrogen atmosphere

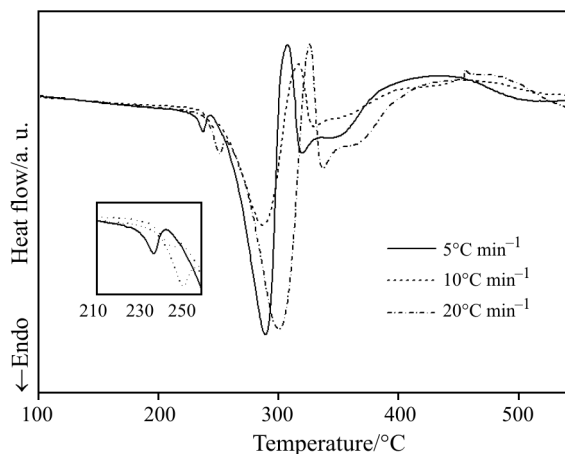


**Fig. 3** DSC curves regarding the thermal decomposition of the  $\text{Ti}(\text{IV})$ –EDTA chelate under nitrogen atmosphere and several heating rates

**Table 1** Data from TG and DSC curves used to obtain the thermal decomposition kinetic parameters  $E$  and  $\log A$  regarding the formation of anhydride and the loss of uncoordinated carboxylate groups of  $\text{Ti}(\text{IV})$ –EDTA complex

Reaction limits							
TG curves				DSC curves			
$\beta/^\circ\text{C min}^{-1}$	start/ $^\circ\text{C}$	stop/ $^\circ\text{C}$	Mass loss/%	$\beta/^\circ\text{C min}^{-1}$	start/ $^\circ\text{C}$	stop/ $^\circ\text{C}$	$\Delta H = \text{J g}^{-1}$
4.98 <sup>a</sup>	215.0	243.0	1.44	5.02 <sup>a</sup>	220.0	242.6	-5.067
4.96 <sup>b</sup>	251.0	301.0	21.6	5.02 <sup>b</sup>	245.4	307.7	-257.7
9.97 <sup>a</sup>	224.9	249.4	1.23	10.05 <sup>a</sup>	224.6	248.4	-2.003
9.88 <sup>b</sup>	254.0	309.4	21.3	10.04 <sup>b</sup>	250.5	316.2	-279.6
20.05 <sup>a</sup>	232.7	253.5	1.01	20.12 <sup>a</sup>	226.3	250.6	-3.575
19.74 <sup>b</sup>	258.8	316.6	21.6	20.03 <sup>b</sup>	252.3	323.6	-329.7

<sup>a</sup>partial of anhydride; <sup>b</sup>loss of uncoordinated carboxylate groups

### Determination of the kinetic model

#### Dollimore's procedure

Dollimore's procedure is applied on the curves TG/DTG whose asymmetry observed between the onset  $T_i$  and the final  $T_f$  in DTG curves, may be associated with the parameters such as the fractional conversion at the peak temperature,  $T_p$ , where is the maximum rate of decomposition,  $\alpha_{\max}$  at  $(d\alpha/dT)_{\max}$ , and the difference between the high-temperature (Hi- $T$ ) and low-temperature (Lo- $T$ ) at half width ( $HW$ ) of the DTG peak,  $HW=Hi-T-Lo-T$ . These parameters can thereby recognize the probable kinetic mechanism expressed as  $f(\alpha)$ .

Through the TG/DTG curves of the Ti(IV)–EDTA complex, Fig. 2, it can calculate these parameters [11, 12], described in Table 2, that indicates the PT,  $f(\alpha)=\alpha(1-\alpha)$ , and R3,  $f(\alpha)=(1-\alpha)^{2/3}$  models [4, 20] to the partial formation of anhydride and the loss of uncoordinated carboxylate groups, respectively. Knowing the averages  $E$  and  $\log A$ ,  $\alpha$ - $T$  relation and  $f(\alpha)$ , the corresponding normalized simulated  $d\alpha/dT$  vs.  $T$  plot could be obtained through Eq. (2) and compared with the normalized experimental DTG curve. The proximity among them indicates the correct kinetic model's determination: PT (Prout–Tompkins), Fig. 4, and R3 (contracting volume), Fig. 5.

Applying the Málek's procedure [4, 9, 10] to the data from DSC curves, Fig. 3, the kinetic models of Ti(IV)–EDTA decomposition could be defined through the  $y(\alpha)$  and  $z(\alpha)$  functions, as defined by the Eqs (9)–(11). The reaction, considering the partial formation of anhydride, presents a maximum of the  $z(\alpha)$  function,  $\alpha_z^*=\alpha_p$ , located at 0.56 (where  $\alpha_p$  is the fractional extent corresponding to the maximum rate  $d\alpha/dt$ , Eq. (7), and the  $y(\alpha)$  function present its maximum,  $\alpha_y^*$ , located at 0.51, Fig. 6a. Their forms with  $\alpha_y^* < \alpha_z^* \leq \alpha_p^*$  is characteristic to the PT model [4]. It is also evident that the PT model is formally identical with the autocatalytic SB (Šesták–Berggren) model in which  $f(\alpha)=\alpha^m(1-\alpha)^n$  when  $m=n=1$ . By this way, the kinetic exponent  $n$  corresponds to the slope of the linear dependence from plot of  $\ln[(d\alpha/dt)\exp(E/RT)]$  vs.

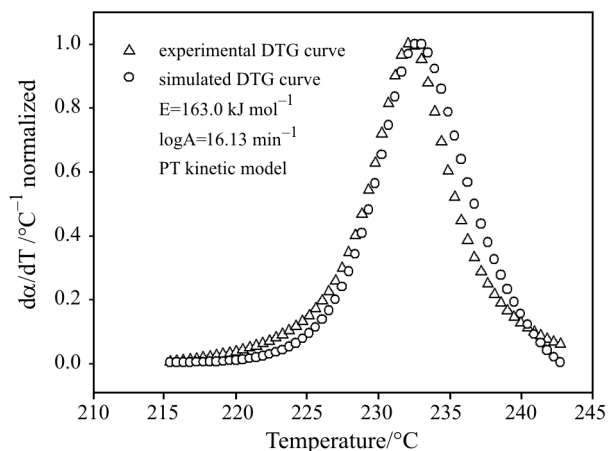


**Fig. 4** Experimental and simulated DTG curves at  $5^\circ\text{C min}^{-1}$  regarding the partial formation of anhydride by Ti(IV)–EDTA chelate decomposition

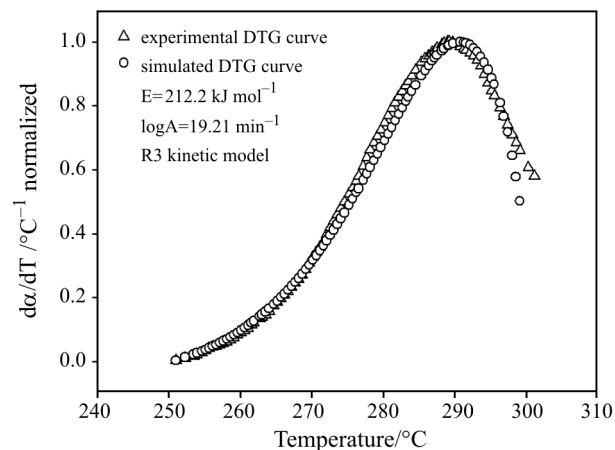


**Fig. 5** Experimental and simulated DTG curves at  $5^\circ\text{C min}^{-1}$  regarding the loss of uncoordinated carboxylate groups by Ti(IV)–EDTA chelate decomposition

$\ln[\alpha^p(1-\alpha)]$  for  $\alpha$  values between 0.2 and 0.8 [21] that yields  $n=1.14$ . The kinetic exponent  $m$  then can be calculated by the relation  $m=pn$  where  $p=\alpha_y^*/(1-\alpha_y^*)$  that yields  $m=1.17$ .

The other reaction, considering the uncoordinated carboxylate groups, present its maximums at  $\alpha_z^*=\alpha_p^*=0.72$  and  $\alpha_y^*=0$  with a convex dependence  $[y(\alpha_1)>\alpha_1]$ , Fig. 6b. This behavior is characteristic to

**Table 2** Data from DTG curves regarding the partial formation of anhydride and the loss of uncoordinated carboxylate groups of Ti(IV)–EDTA complex

Anhydride				Carboxylate			
$\beta/^\circ\text{C min}^{-1}$	$T_{\text{peak}}/^\circ\text{C}$	$\alpha_{\max}$	HW	$\beta/^\circ\text{C min}^{-1}$	$T_{\text{peak}}/^\circ\text{C}$	$\alpha_{\max}$	HW
4.98	232.6	0.50	6.50	4.96	289.2	0.61	26.43
9.97	243.0	0.59	9.63	9.88	298.6	0.61	26.69
20.05	246.0	0.57	10.06	19.74	311.0	0.69	23.62
expected to PT		$0.5 \leq \alpha \leq 0.6$	–	expected to R3*		$0.6 \leq \alpha \leq 0.7$	20–42

HW=half width of DTG peak; \* $T_i$ =diffuse and  $T_f$ =sharp

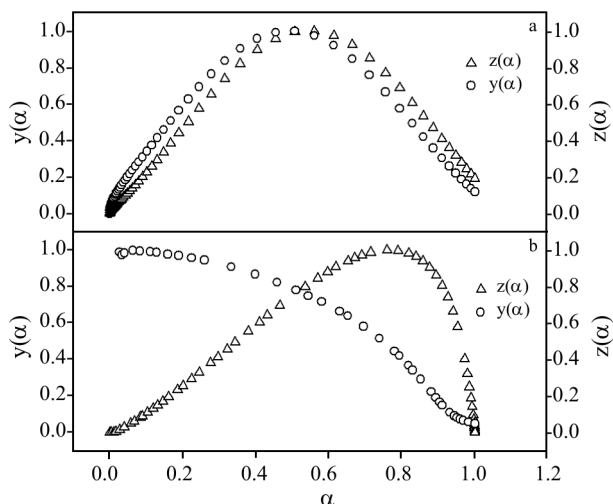


**Fig. 6** The  $y(\alpha)$  and  $z(\alpha)$  functions calculated from DSC data (Fig. 3) regarding the a – partial formation of anhydride and b – thermal decomposition of the carboxylate groups

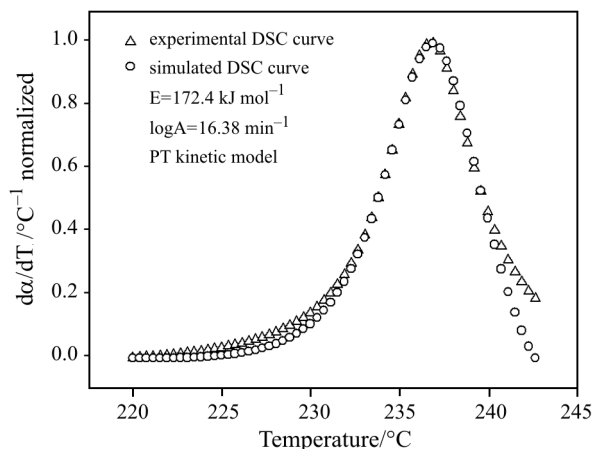


**Fig. 7** Experimental and simulated DSC curves at  $5^\circ\text{C min}^{-1}$  regarding the partial formation of anhydride by Ti(IV)–EDTA chelate

the RO model,  $f(\alpha)=(1-\alpha)^n$ , for  $n < 1$  [4]. In this case, the kinetic exponent  $n \neq 0$  can be calculated iteratively using the equation

$$\alpha_z^* = 1 - \left[ 1 + \frac{1-n}{n} x_p \pi(x_p) \right]^{\frac{1}{(n-1)}}$$

where  $\pi(x_p)=1/(x_p+2)$  and  $x_p=E/RT_p$  at peak temperature from DSC [21].

This equation establishes the dependence of the maximum rate ( $d\alpha/dt$ ),  $\alpha_p^*$ , on the kinetic exponent  $n$  that can be designed from plot of  $\alpha_p$  vs.  $n$ . Thus, for RO( $n$ ) model's decarboxylation reaction,  $n$  is determined by interpolation of  $\alpha_p^*=0.72$  in this dependence. The found value to  $n$  is 0.61.

The normalized simulated  $\phi$  vs.  $T$  plot obtained through Eq. (8) and its proximity with the experimen-

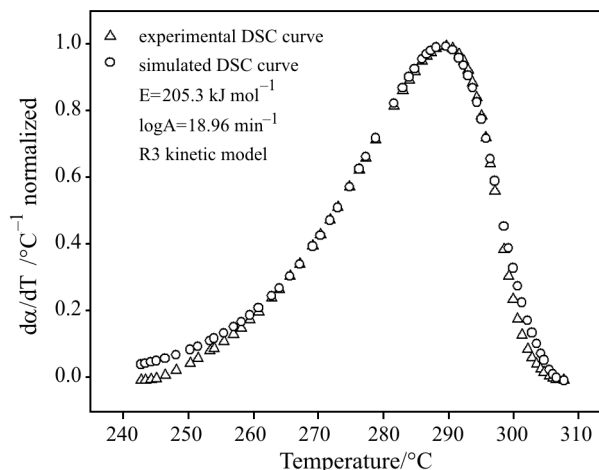


**Fig. 8** Experimental and simulated DTG curves at  $5^\circ\text{C min}^{-1}$  regarding the loss of uncoordinated carboxylate groups from Ti(IV)–EDTA chelate

tal DSC curves indicates the PT, in which the process is controlled by nucleation with branching nuclei interacting during their growth,  $f(\alpha)=\alpha^{1.17}(1-\alpha)^{1.14}$ , Fig. 7, and R3, which is a phase-boundary controlled reaction [22],  $f(\alpha)=(1-\alpha)^{0.61}$ , Fig. 8, as the correct kinetic models to the solid-state process for anhydride and decarboxylation reaction, respectively, according to these found by Dollimore's procedure.

## Conclusions

TiO(NCH<sub>2</sub>(CH<sub>2</sub>COO)<sub>2</sub>H)<sub>2</sub> compound shows itself as a pentacoordinated chelate having two uncoordinated carboxylate group. The loss of the thermally weaker uncoordinated carboxylate groups happened in two steps, the first one showing the formation of anhydride compound following the Prout–Tompkins (PT) model, and the second one indicating the loss of the carboxylate groups following the 3-D interface reaction. Previous work in our group regarding the thermal decomposition of Sn-EDTA heptacoordinated chelate [23] had showed the loss of coordinated water and thermal decomposition of carboxylate group following the R3 and SB model, respectively. Besides the strong kinetic dependence on the experimental condition in a dynamic procedure, it can be seen from the resemblance between simulated and experimental normalized DTG and mainly DSC curves.

## Acknowledgements

The authors acknowledge Capes and Fapesp (proc. 02/05935-3) for the financial support of this work.

**References**

- 1 D. T. Sawyer and J. M. McKinnie, *J. Am. Chem. Soc.*, **82** (1960) 4191.
- 2 F. J. Kristine, R. E. Shepherd and S. Siddiqui, *Inorg. Chem.*, **20** (1981) 2571.
- 3 J. P. Fackler, F. J. Kristine, A. M. Mazany, T. J. Moyer and R. E. Shepherd, *Inorg. Chem.*, **24** (1985) 1857.
- 4 J. Málek, T. Mitsuhashi and J. M. Criado, *J. Mater. Res.*, **16** (2001) 1862.
- 5 J. H. Flynn and L. A. Wall, *J. Res. Nat. Bur. Stand., A*, **70** (1966) 487.
- 6 S. Vyazovkin and C. A. Wight, *Int. Rev. Phys. Chem.*, **17** (1998) 407.
- 7 J. H. Flynn and L. A. Wall, *J. Polym. Sci., Pt. B*, **4** (1966) 323.
- 8 C. D. Doyle, *J. Appl. Polym. Sci.*, **5** (1961) 285.
- 9 J. Málek, *J. Therm. Anal. Cal.*, **56** (1999) 763.
- 10 J. Málek, *Thermochim. Acta*, **355** (2000) 239.
- 11 D. Dollimore, T. A. Evans, Y. F. Lee and F. W. Wilburn, *Thermochim. Acta*, **188** (1991) 77.
- 12 D. Dollimore, T. A. Evans, Y. F. Lee, G. P. Pee and F. W. Wilburn, *Thermochim. Acta*, **196** (1992) 255.
- 13 R. K. Sharma and M. C. Bhatnagar, *Sens. Actuators B*, **56** (1999) 215.
- 14 G.-J. Li, X.-H. Zhang and S. Kawi, *Sens. Actuators B*, **60** (1999) 64.
- 15 B. Karadakov and P. Nenova, *J. Inorg. Nucl. Chem.*, **33** (1971) 2541.
- 16 M. F. G. Esteban, R. V. Serrano and F. G. Vilchez, *Spectrochim. Acta, Part A*, **43A** (1987) 1039.
- 17 D. T. Sawyer and P. J. Paulsen, *J. Am. Chem. Soc.*, **81** (1959) 816.
- 18 A. A. McConnel and R. H. Nuttall, *Spectrochim. Acta, Part A*, **33A** (1977) 459.
- 19 T. R. Bhat and R. K. Iyer, *J. Inorg. Nucl. Chem.*, **29** (1967) 179.
- 20 D. Chen, X. Gao and D. Dollimore, *Thermochim. Acta*, **215** (1993) 109.
- 21 J. Málek, *Thermochim. Acta*, **200** (1992) 257.
- 22 J. Šesták and G. Berggren, *Thermochim. Acta*, **3** (1971) 1.
- 23 L. S. Guinesi, C. A. Ribeiro, M. S. Crespi and A. M. Veronezi, *Thermochim. Acta*, **414** (2004) 35.

---

Received: March 31, 2005

Accepted: July 4, 2005

OnlineFirst: December 12, 2005

---

DOI: 10.1007/s10973-005-7027-7